DOI: 10.13009/EUCASS2022-4673

Numerical assessment of RANS and LES modelling in particle separation devices

L. Bahramian, A. Amani*, J. Muela**, J. Rigola*, C. Oliet*, and C.D. Pérez-Segarra*†*
**Heat and Mass Transfer Technological Center (CTTC), Universitat Politècnica de Catalunya-BarcelonaTech(UPC),*
ESEIAAT, Colom 11, 08222, Terrassa (Barcelona), Spain.
***Termo Fluids S.L., Av. Jacquard 97-E, 08227, Terrassa (Barcelona), Spain.*
linda.bahramian@upc.edu , cdavid.perez.segarra@upc.edu
† Corresponding author

Abstract
In the present work, the separation efficiency analysis on particle-laden flows in the framework of LES and RANS modelling for an Inertial Particle Separator (IPS) device has been presented. The comparison of LES and RANS will allow us to study and assess both the advantages and disadvantages of these modelling techniques for the design and optimisation purposes of IPS devices. The results show that RANS modelling can yield similar results on the aggregate level with a comparably lower computational cost.

1. Introduction

One of the most critical challenges of the aerospace industry nowadays and in the upcoming years is the reduction of pollutant gas emissions. The final aim is the design of All Electric Aircraft (AEA) with zero-emission. Nonetheless, fully electric flights are still a long way in the future since there are many challenging aspects to be faced before they become a reality [1]. Meanwhile ,the More Electrical Aircraft (MEA) is the bridge between current aircraft and AEA. The main idea of MEA is to substitute all non-propulsive systems with fully electric-powered systems [2], one of which is the Environmental Control System (ECS). This system is devoted to maintaining the temperature and air pressure in the comfort range within the cabin. Conventionally, the inlet air required for feeding the compressors of the ECS is obtained by bleeding air from the latter stages of the compressors of the engine aircraft, which guarantees the supply of clean air without Foreign Object Debris (FOD). Nonetheless, this bleeding induces an additional fuel burn and can lead to the ingestion of potential harmful neurotoxic substances [3]. Aiming to avoid the issues of this air-bleeding , MEA is designed to use a new Electrical Environmental Control System (EECS), which is directly fed with air coming from the ambient atmosphere. The problem is that this air may contain FOD, which can dramatically reduce the service life of the compressor, if not directly damage it. Therefore, in order to minimise this risk, a protection system against this FOD must be employed before the compressor of the EECS. Inertial Particle Separator (IPS) devices are very well-suited candidates to be part of reliable FOD protection systems for EECS [4]. These IPS devices have to be designed to guarantee the required FOD protection and yield the minimum pressure loss.
Computational Fluid Dynamics (CFD) can be a powerful tool for designing and optimising IPS devices. Due to limited computational resources, performing Direct Numerical Simulations (DNS) of turbulent flows where all the temporal and length scales of the flow must be solved is restricted to relatively simple academical cases. Therefore, the turbulence modelling technique should be employed for the design and optimisation of IPS devices. The two most common turbulence modelling techniques are Reynolds-Average Navier-Stokes (RANS) and Large Eddy Simulation (LES). It is known by the research community that LES offers a higher degree of accuracy compared to RANS at the expense of higher computational costs. The flow pattern found in IPS devices can be really complex, and its resolution can highly affect the calculated flow-particle interactions. Therefore, it is of interest to study and assess the capabilities and limitations of both modelling techniques in the simulation of IPS devices.
This paper is organised as follows: First, in section 2, the mathematical description of dispersed multi-phase turbulent flows using an Eulerian-Lagrangian (EL) approach in LES and RANS is detailed. Then, in section 3, the test case, the numerical set-up, mesh, and boundary conditions employed to carry out the simulations are described. In section 4, the

DOI: 10.13009/EUCASS2022-4673

results are presented for different wall collision models and flow Reynolds numbers. The results obtained for each of these aspects are examined and studied. Finally, conclusions remarks are discussed in section 5.

2. Mathematical model

Simulations of dispersed multiphase flows involve the resolution of both continuous and dispersed phases. Among the different numerical methods available to simulate these kinds of flows [5], in the present work, the Eulerian-Lagrangian approach has been employed [6]. It is based on a point-particle approach, where particles or groups of identical particles, known as parcels, are tracked individually throughout all the computational domains. Hence, this method represents the dispersed phase by employing a Lagrangian reference framework, while the continuous phase is solved using the classical Eulerian frame. Moreover, the continuous phase is solved by Large Eddy Simulation (LES) and Reynolds Averaged Navier-Stokes (RANS). Although LES is computationally more expensive than RANS approach, it can capture the unsteadiness and complexity of the flow patterns. Following, the governing equations describing both continuous and dispersed phases are detailed.

2.1 Continuous phase

The equations of a viscous incompressible continuous fluid with constant properties are governed by the Navier-Stokes (NS) equations [7].

$$\frac{\partial u_i}{\partial t}+\frac{\partial}{\partial x_j}\left(u_i u_j\right)=-\frac{1}{\rho}\frac{\partial p}{\partial x_i}+\nu\frac{\partial}{\partial x_j}\left(\frac{\partial u_i}{\partial x_j}+\frac{\partial u_j}{\partial x_i}\right), \qquad i=1,2,3 \tag{1}$$

$$\frac{\partial u_i}{\partial x_i}=0 \tag{2}$$

where t represents time, ρ is the density, u is the velocity vector, p stands for the pressure, and υ is kinematic viscosity. In order to better implement the Navier-Stokes equations in LES and RANS modelling, they can be written in the filtered form. In light of the commutation with derivation property, the application of a filter to Eq. (1) and Eq. (2) is expressed as:

$$\frac{\partial \overline{u}_i}{\partial t}+\frac{\partial}{\partial x_j}\left(\overline{u_i u_j}\right)=-\frac{1}{\rho}\frac{\partial \overline{p}}{\partial x_i}+\nu\frac{\partial}{\partial x_j}\left(\frac{\partial \overline{u}_i}{\partial x_j}+\frac{\partial \overline{u}_j}{\partial x_i}\right) \tag{3}$$

$$\frac{\partial \overline{u}_i}{\partial x_i}=0 \tag{4}$$

where $\bar{p}$ is the filtered pressure. The filtered momentum equation brings out the non-linear term $\overline{u_i u_j}$, which can be expressed as a function of $\bar{u}$ and u' where:

$$u'=u-\overline{u} \tag{5}$$

Leonard [8] expressed the non-linear term in the form of a triple summation:

DOI: 10.13009/EUCASS2022-4673

$$\overline{u_i u_j} = \overline{(\overline{u}_i + u_i')(\overline{u}_j + u_j')} = \overline{\overline{u}_i \overline{u}_j} + \overline{\overline{u}_i u_j'} + \overline{\overline{u}_j u_i'} + \overline{u_i' u_j'} \quad \textbf{(6)}$$

In LES modelling, the larger scale flow characteristics are solved, while the subgrid-scales (SGS) are modelled. This scale separation is obtained by applying a low-pass filter to the transport equations [9]. For incompressible flows with constant viscosity ,the filtered momentum equation is then expressed as:

$$\frac{\partial \overline{u}_i}{\partial t} + \frac{\partial}{\partial x_j}\left(\overline{\overline{u}_i \overline{u}_j}\right) = -\frac{1}{\rho}\frac{\partial \overline{p}}{\partial x_i} + \nu \frac{\partial}{\partial x_j}\left(\frac{\partial \overline{u}_i}{\partial x_j} + \frac{\partial \overline{u}_j}{\partial x_i}\right) - \frac{\partial \tau_{ij}}{\partial x_j} \quad \textbf{(7)}$$

in which the subgrid tensor τ, grouping together all the terms that are not exclusively dependent on the large scales, must be modelled to close Eq. (3). In the present work, this term is closed by employing an eddy-viscosity-type model following the Boussinesq hypothesis defined as [7]:

$$\tau_{ij} = C_{ij} + R_{ij} = \overline{u_i u_j} - \overline{\overline{u}_i \overline{u}_j} \quad \textbf{(8)}$$

where the cross-stress tensor, C, which represents the interactions between large and small scales, and the Reynolds subgrid tensor R, which reflects the interaction between subgrid scales, are expressed as:

$$C_{ij} = \overline{\overline{u}_i u_j'} + \overline{\overline{u}_j u_i'} \quad \textbf{(9)}$$

$$R_j = \overline{u_i' u_j'} \quad \textbf{(10)}$$

In Reynolds-Average Navier-Stokes (RANS), subgrid tensor τ reduces to [10]:

$$\tau_{ij} = R_{ij} = \overline{u_i' u_j'} \quad \textbf{(11)}$$

where R is the Reynolds-stress tensor that incorporates the effects of turbulent motions on the mean stresses.

2.2 Dispersed phase

As mentioned before, the dispersed phase is modelled employing a Lagrangian reference framework. The motion of particles and droplets in a fluid using a Lagrangian framework can be described by classical equations of motion, i.e., Newton's law. The first authors to work and develop a model for the dispersed phase using this approach were Basset [11], Boussinesq [12] and Oseen [13]. Hence, the equation of motion for particles derived from their work is known as the BBOequation. This BBO-equation was extended to non-uniform flows for small rigid particles by Maxey and Riley [14]. In general ,the ordinary differential equations required to describe the behaviour of the dispersed phase are:

$$\frac{\mathrm{d}\mathbf{x_p}}{\mathrm{d}t} = \mathbf{v_p} \quad \textbf{(12)}$$

$$m_\mathrm{p}\frac{\mathrm{d}\mathbf{v_p}}{\mathrm{d}t} = \sum_i \mathbf{F_i} \quad \textbf{(13)}$$

where m_p is the particle's mass, v_p the particle's velocity, x_p is the particle's position and $\sum_i F_i$ is the sum of all the relevant forces acting over the particle.

DOI: 10.13009/EUCASS2022-4673

3. Test case description

The selected test case is an Inertial Particle Separator (IPS) device. IPS devices achieve the separation of particles from the core flow by varying the particles' velocity – either in direction or magnitude – such that a response lag is introduced between the particles and fluid. Particles are separated by the drift away from the original streamline under their own inertia. Thus, a common feature of all IPS ducts is a flow path with a curvature. A correctly functioning IPS bifurcates the flow after the hump into two channels; core and scavenge. The core channel should be designed to have a smaller concentration of particles compared with the scavenge channel. To do this, a portion of the inlet mass flow must exit through the scavenge channel along with the separated particles. The majority of the separation occurs in the bifurcation zone, where the most severe change in direction occurs. Hence, one of the interesting parameters to compare in different numerical simulations can be an estimation of the concentration change between the core and scavenge flow channel, i.e. the separation efficiency, defined as the mass of particles leaving the scavenge channel divided by the total mass of the injected particles. In the present work, to have a comparison between RANS and LES, the separation efficiency of the particles for two Reynolds numbers using two distinct particle-wall collisions models is calculated. Fig. 1 illustrates a schematic representation of a simplified particle separator with a scavenge mass flow rate ratio of 10%.

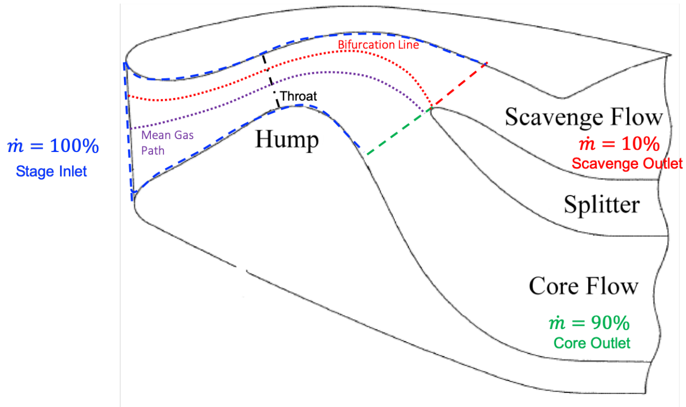

Figure 1: Simplified particle separator geometry

The foreign object debris (FOD) can be presented in various sizes and natures, such as gravel, runway debris, water, sand, etc. Sand ingestion can be a result of operations around dusty airports or flights through dust plumes, while water may enter the engine in the form of ice, snow, rain, inlet condensation, droplet suspension, or liquid spray. The intake is positioned in such a way that it is at risk of ingesting runway debris thrown up by aircraft tires or washed up by the thrust reverser jet impinging on the runway.

3.1 Numerical setup

All the numerical simulations performed in this work have been carried out using the open-source code OpenFOAM [15], based on the finite volume method (FVM). For dispersed phase, one-way coupling Lagrangian method and for continuous phase Eulerian methodis applied.

As mentioned in section 2.1, the term τ^R must be closed through a turbulence model. Muela, J. et al. [16] have compared three different turbulence models for an IPS device. The first model was the Smagorinsky [17] based on the Prandtl mixing length applied to SGS modelling. The second one was the Wall-adapting eddy viscosity model (WALE) SGS model developed by Nicoud [18]. In the third one, the variational multiscale (VMS) approach was applied to the WALE. However, this approach originally formulated for Smagorinsky model by Hughes [19]. According to them, the Smagorinsky model yielded dissipative behaviours close to the walls, generating a very large boundary layer. Both WALE and VMS models presented very similar results, and both were able to properly model the flow close to the walls, which are crucial when simulating confined flows, similar to the one of the present work. Therefore, the WALE model is selected for the turbulence model carried out in this work.

In the LES simulations, the simulation is run for two flow-throughs before the averaging process is started. Afterwards, the mean values of the fields are averaged for three flow-throughs. For RANS cases, the simulations were running as long as needed to reach the steady-state.

DOI: 10.13009/EUCASS2022-4673

3.2 Mesh

The favourable geometry has allowed the utilisation of a structured mesh, as depicted in Fig. 2. Different meshes have been applied with varying numbers of control volumes. In LES, one needs a refined mesh, especially closer to the walls and in regions with more complicated flow patterns. A mesh sensitivity analysis was performed, and a structured mesh with 9 million control volumes (CVs) was selected as the final candidate.

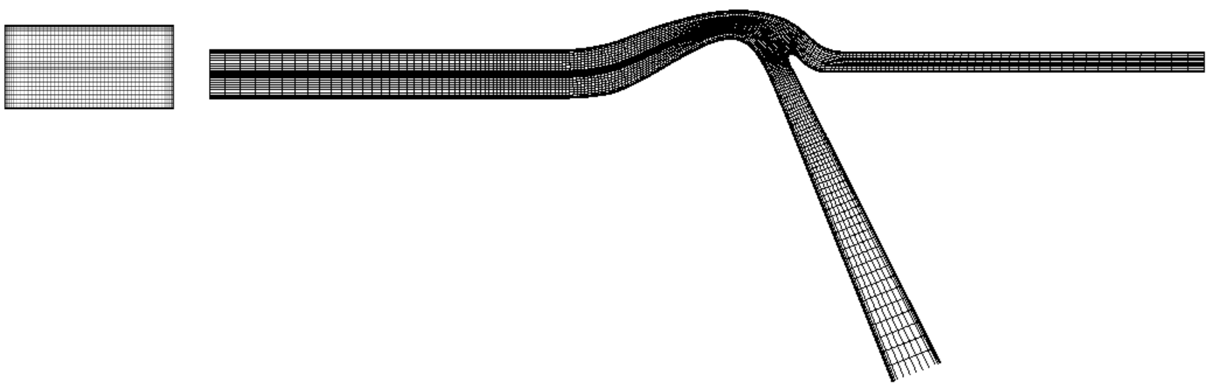

(a) Plane YZ (b) Plane XY

Figure 2: Mesh scheme of computational domain

3.3 Boundary conditions

The boundary conditions (BCs) have a crucial role in numerical simulations, especially in the geometry inlet of LES modelling. A comparison between different inlet boundary conditions in the context of LES is carried out by Montorfano et al. [20]. However ,it is sometimes difficult to exactly produce the desired turbulent BCs at the inlet . Different approaches can be used for producing turbulence inlet boundary conditions in OpenFOAM ,such as white noise (which dissipates extremely quickly), synthetic turbulent generators (which require experimental data as input), extended inlet (which requires a large extension of the inlet, usually the order of 10-20 channel height), and plane mapping.

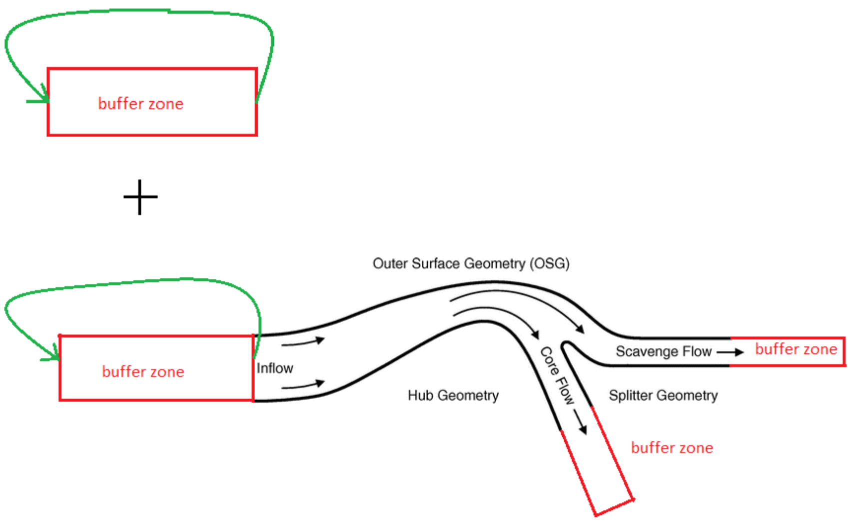

Figure 3: schematic representation of the implemented inlet and outlet boundary conditions

DOI: 10.13009/EUCASS2022-4673

Thus, to produce an appropriate turbulent inlet boundary condition with the least computational costs possible, first, an extended inlet with the length of 4-6 orders of inlet height has been solved separately, with periodic boundary conditions in the flow direction. Then, this extended inlet is located upstream of the main inlet by mapping the fields obtained on its whole domain. In the final step, the simulation is carried out using a periodic boundary condition just for the extended inlet part to generate a turbulent inlet for each time step. A schematic representation of these procedures is shown in Fig. 3.
Also, it is suggested to use an extended outlet zone to avoid facing a divergence in the outlet and also increase the viscosity in that zone to smooth out the turbulent patterns exiting the domain.

3.4 Particle-wall collision

Another critical aspect of the study of IPS devices is defining the suitable particle-wall collision model according to the roughness of the wall and particle shapes. An ideal approach is to consider an elastic collision model which treats all the surfaces as ideally smooth with no roughness. So, with this approach, the kinetic energy of the particles remains constant during and after colliding with the wall. But this is not the case in IPS materials, where the collisions of particles with the wall are inelastic, and the surfaces have a certain amount of roughness. In the present work, two particle-wall collision models have been employed, an elastic model and an inelastic particle-wall collision model presented by Taslim et al. [21]. Particle bounce is usually modelled using equations for average restitution coefficients and standard deviations. These equations are either based on the ratio of normal and tangential velocities before and after the impact and the ratio of incidence and rebound angles (all as a function of incidence angle) or the ratio of velocity vectors before and after the impact and the ratio of incidence and rebound angles. The inelastic model presented by Taslim et al. [21] is as follows:

$$\begin{aligned}\text{Restitution Coefficient} &= \text{(Rebound/Initial)}\\ &= K_1 + K_2\beta_1 + K_3\beta_1^2 + K_4\beta_1^3 + K_5\beta_1^4\end{aligned} \tag{14}$$

$$\begin{aligned}\text{Standard Deviation} &= \text{(Deviation/Initial)}\\ &= \mathrm{C}_1 + C_2\beta_1 + C_3\beta_1^2 + C_4\beta_1^3 + C_5\beta_1^4\end{aligned} \tag{15}$$

For the aluminium target surface, which is normally used in IPS devices, the coefficients for the polynomials of Eqs. (14) and (15) are:

$$\frac{V_2}{V_1} = 1 - 2.03\beta_1 + 3.32\beta_1^2 - 2.24\beta_1^3 + 0.472\beta_1^4 \tag{16}$$

$$\frac{\beta_2}{\beta_1} = 1 + 0.409\beta_1 - 2.52\beta_1^2 + 2.19\beta_1^3 - 0.531\beta_1^4 \tag{17}$$

$$\frac{V_{n_2}}{V_{n_1}} = 0.993 - 1.76\beta_1 + 1.56\beta_1^2 - 0.49\beta_1^3 \tag{18}$$

$$\frac{V_{t_2}}{V_{t_1}} = 0.988 - 1.66\beta_1 + 2.11\beta_1^2 - 0.67\beta_1^3 \tag{19}$$

4. Results

In this section, the results obtained for RANS and LES for the IPS device described in the previous section are presented.

DOI: 10.13009/EUCASS2022-4673

4.1 First test case

The first test case is carried out with the Reynolds number of 50000 and the scavenge mass flow rate ratio of 15% in the framework of RANS and LES for two particle-wall collisions of elastic and inelastic models. Fig. 4 illustrates the cross-section mean velocity value for RANS and LES. As can be seen in Fig. 5 and Fig. 6, the separation efficiencies of particles for RANS and LES are in good agreement.

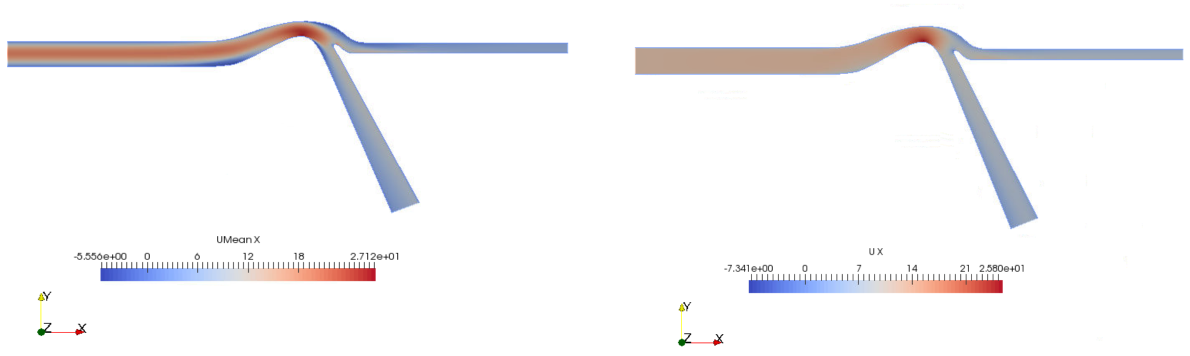

(a) (b)

Figure 4: The cross-section velocity contours of (a) LES and (b) RANS for Reynolds number of 50000 with scavenge mass flow rate ratio of 15%

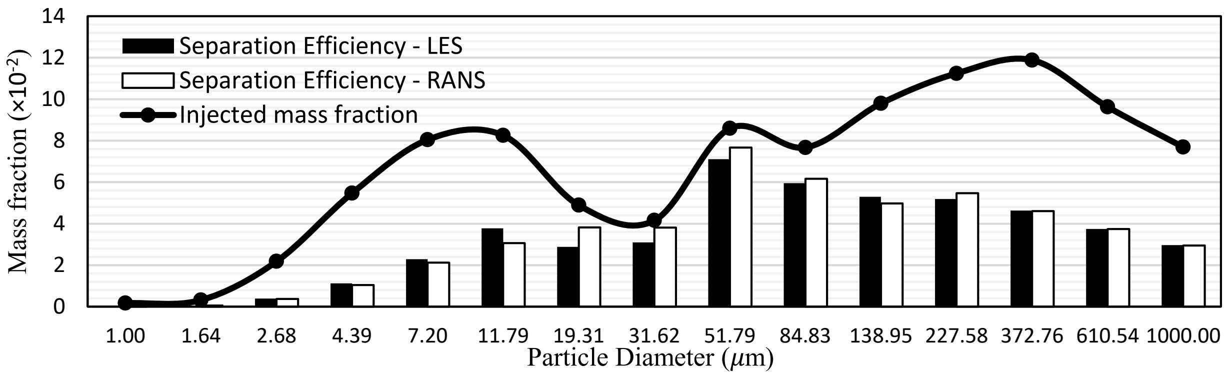

Figure 5: The separation efficiencies for RANS and LES in Re=50000 with scavenge mass flow rate ratio=15% and elastic wall collision

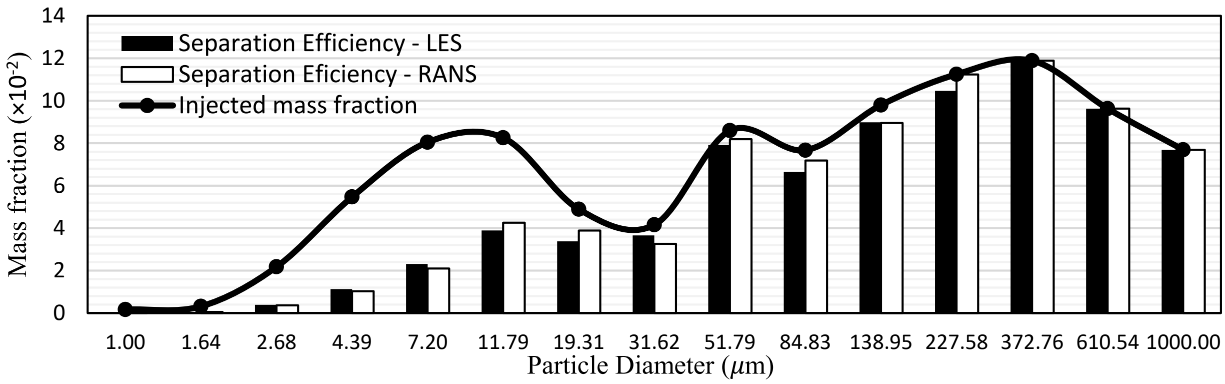

Figure 6: The separation efficiency for RANS and LES in Re=50000 with scavenge mass flow rate ratio=15% and inelastic wall collision

DOI: 10.13009/EUCASS2022-4673

4.2 Second test case

The second test case is simulated with the Reynolds number of 25000 and the scavenge mass flow rate ratio of 15% in the framework of RANS and LES for two particle-wall collisions of elastic and inelastic models. As shown in Fig. 7 and Fig. 8, the separation efficiencies of particles for RANS and LES models are in good agreement. The computational cost calculated in this case for RANS was 191 CPU-hour and for LES, 4423 CPU-hour.

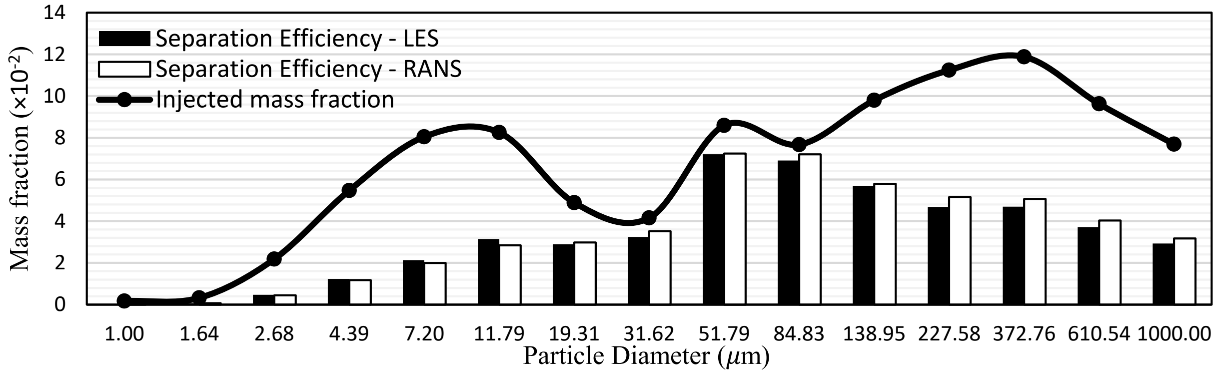

Figure 7: The separation efficiency for RANS and LES in Re=25000 with scavenge mass flow rate ratio=15% and elastic wall collision

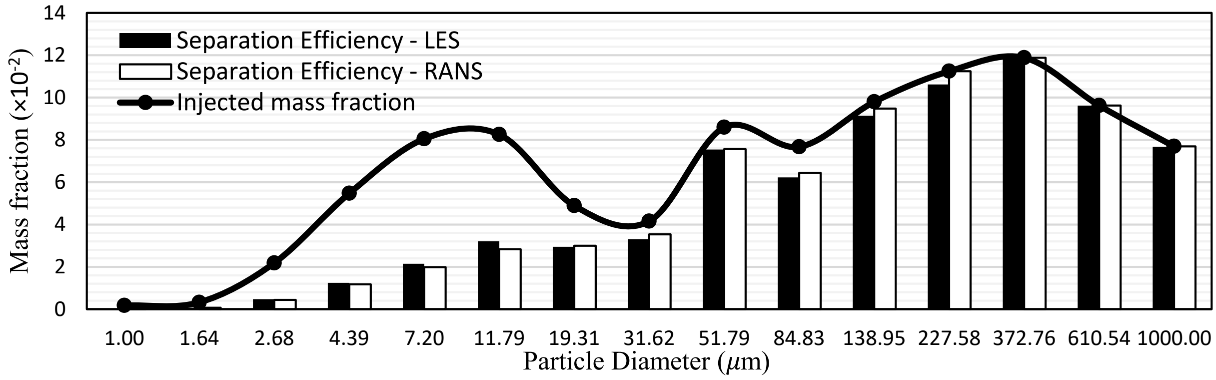

Figure 8: The separation efficiency for RANS and LES in Re=25000 with scavenge mass flow rate ratio=15% and inelastic wall collision

5. Conclusions

Numerical simulations are one of the powerful tools for the design and optimisation of Foreign Object Debris (FOD) protection and separation devices. IPS are devices designed to separate and remove Foreign Object Debris (FOD) at the inlet of systems such as the turbo-compressor of EECS in aircraft. The objective of this work was not to compare the flow pattern of RANS vs. LES but to evaluate the similarities of the yielded particle separation results obtained from these two approaches. Separation efficiencies for two particle-wall collision models of elastic and inelastic in two different Reynolds numbers were extracted from both RANS and LES simulations. The results show a good agreement between the separation efficiency extracted from these two approaches. Keeping in mind the comparably higher computational cost required for LES simulations, on the aggregate level, especially in the design stage of IPS devices, the RANS turbulent modelling with much lower computational cost, can be a good substitute for LES.

6. Acknowledgements

This work has been developed within the EU H2020 Clean Sky 2 research project "A New proTection devIce for FOD - ANTIFOD" (grant agreement Nº 821352).

DOI: 10.13009/EUCASS2022-4673

Linda Bahramian acknowledges the financial support from the Secretariat of Universities and Research of the Generalitat de Catalunya and the European Social Fund, FI AGAUR Grant (2019 FI_B 01205).
Carles Oliet, as a Serra Húnter lecturer, acknowledges the Catalan Government for the support through this Programme.

References

[1] Wheeler, P. 2016. Technology for the more and all electric aircraft of the future. *IEEE International Conference on Automatica (ICA-ACCA).* 1-5.
[2] Sarlioglu, B., and Morris, C.T. 2015. More electric aircraft: Review, challenges, and opportunities for commercial transport aircraft. *IEEE Transactions on Transportation Electrification, 1*(1): 54-64.
[3] Sinnett, M., 2007. 787 no-bleed systems: saving fuel and enhancing operational efficiencies. *Aero Quarterly*, 18: 6-11.
[4] Filippone,A. and Bojdo, N. 2010. Turboshaft engine air particle separation. *Progress in Aerospace Sciences*, 46(5-6): 224-245.
[5] Sommerfeld, M. ed. 2008. Best Practice Guide-line for Computational Fluid Dynamics of Dispersed Multi-Phase Flows. *European Research Community on Flow, Turbulence and Combustion (ERCOFTAC)*.
[6] Subramaniam, S. 2013. Lagrangian-Eulerian methods for multiphase flows. *Progress in Energy and Combustion Science,* 39(2-3): 215-245.
[7] Sagaut, P. 2006. Large Eddy Simulation for Incompressible Flows: An Introduction. *Scientific Computation. Springer.*
[8] Leonard, A. 1975. Energy cascade in large-eddy simulations of turbulent fluid flows. In *Advances in geophysics*. 18:237-248 Elsevier.
[9] Pope, S.B. 2011. Turbulent flows. *Cambridge Univ. Press.*
[10] Alfonsi, G. 2009. Reynolds-Averaged Navier-Stokes Equations for Turbulence Modeling, *Applied Mechanics Review*. 62(4).
[11] Basset, A.B. 1888. On the motion of a sphere in a viscous liquid. *Philosophical Transactions of the Royal Society of London A: Mathematical, Physical and Engineering Sciences.* 179:43-63.
[12] Boussinesq, J. 1885. Sur la résistance qu'oppose un liquide indéfini en repos. *CR Acad. Sci. Paris.* 100:935-937.
[13] Oseen, C. W. 1927. Hydrodynamik. *Akademische Verlag, Leipzig*.
[14] Maxey, M.R. and Riley, J.J. 1983. Equation of motion for a small rigid sphere in a nonuniform flow. *Physics of Fluids.* 26:883-889.
[15] OpenCFD 2019. OpenFOAM – The Open Source CFD Toolbox – User's Guide, OpenCFD Ltd.
[16] Muela Castro, J., Rigola Serrano, J., Oliet Casasayas, C., Pérez Segarra, C. D., and Oliva Llena, A. 2019. Assessment of numerical aspects using LES in particle separation devices. In *8th European Conference for Aeronautics and Space Science (EUCASS): papers*. 1-15. European Conference for AeroSpace Sciences (EUCASS).
[17] Smagorinsky, J. 1963. General circulation experiments with the primitive equations: I. The basic experiment. *Monthly weather review.* 91(3): 99-164.
[18] Nicoud, F. and Ducros, F.1999. Subgrid-scale stress modelling based on the square of the velocity gradient tensor. *Flow, turbulence and Combustion.* 62(3): 183-200.
[19] Hughes, T.J., Mazzei, L., and Jansen, K.E. 2000. Large eddy simulation and the variational multiscale method. *Computing and Visualization in Science.* 3(1): 47-59.
[20] Montorfano, A., Piscaglia, F. and Ferrari, G. 2013. Inlet boundary conditions for incompressible LES: Acomparative study. *Mathematical and computer Modeling.* 57: 1640-1647.
[21] Taslim, M.E., Khanicheh, A., and Spring, S. 2009. A numerical study of sand separation applicable to engine inlet particle separator systems. *Journal of the American Helicopter Society*. 54(4): 42001-42001.